Eur. Phys. J. D **41**, 325–330 (2007)
DOI: 10.1140/epjd/e2006-00220-2

THE EUROPEAN PHYSICAL JOURNAL D

Frenkel-Kontorova model with cold trapped ions

I. García-Mata[1], O.V. Zhirov[2], and D.L. Shepelyansky[1,a]

[1] Laboratoire de Physique Théorique, UMR 5152 du CNRS, Univ. P. Sabatier, 31062 Toulouse Cedex 4, France
[2] Budker Institute of Nuclear Physics, 630090 Novosibirsk, Russia

Received 26 June 2006 / Received in final form 24 August 2006
Published online 27 September 2006 –

Abstract. We study analytically and numerically the properties of one-dimensional chain of cold ions placed in a periodic potential of optical lattice and global harmonic potential of a trap. In close similarity with the Frenkel-Kontorova model, a transition from sliding to pinned phase takes place with the increase of the optical lattice potential for the density of ions incommensurate with the lattice period. We show that at zero temperature the quantum fluctuations lead to a quantum phase transition and melting of pinned instanton glass phase at large values of dimensional Planck constant. After melting the ion chain can slide in an optical lattice. The obtained results are also relevant for a Wigner crystal placed in a periodic potential.

PACS. 32.80.Lg Mechanical effects of light on atoms, molecules, and ions – 32.80.Pj Optical cooling of atoms; trapping – 63.70.+h Statistical mechanics of lattice vibrations and displacive phase transitions – 61.44.Fw Incommensurate crystals

1 Introduction

Nowadays experimental techniques allow to store thousands of cold ions and observe various ordered structures formed by Coulomb repulsion in ion traps [1]. These structures include the one-dimensional (1D) Wigner crystal, zig-zag and helical structures in three dimensions. The Cirac-Zoller proposal of quantum computations with cold trapped ions [2] generated an enormous experimental progress in this field with implementations of quantum algorithms and quantum state preparation with up to 8 qubits [3,4]. In these experiments [3,4] ions form a 1D chain placed in a global harmonic potential which frequency ω determines the eigenfrequencies of chain oscillations being independent of ion charge [5,6]. Highly accurate experimental control of the chain modes allows to perform quantum gates between internal levels of ions. In addition to ion traps, modern laser techniques allow to create periodic optical lattices and store in them thousands of cold atoms (see e.g. [7]). A single ion dynamics in an optical lattice has been also studied experimentally [8]. The combination of these two techniques makes possible to study experimentally the properties of a 1D chain of few tens of ions placed in an optical lattice and a global harmonic potential at ultra low temperatures.

In this paper we analyze the physical properties of such a system and show that it is closely related to the Frenkel-Kontorova Model (FKM) [9] which gives a mathematical description of various physical phenomena including crystal dislocations, commensurate-incommensurate phase transitions, epitaxial monolayers on a crystal surface, magnetic chains and fluxon dynamics in Josephson junctions (see [10] and references therein). As in the classical FKM the ion chain exhibits the Aubry analyticity breaking transition [11] when the amplitude of optical potential becomes larger than a certain critical value. Below the critical point the classical chain can slide (oscillate) in the incommensurate optical lattice while above the transition it becomes pinned by the lattice and a large gap opens in the spectrum of phonon excitations. Above the transition the positions of ions form a devil's staircase corresponding to a fractal Cantor set which replaces a continuous Kolmogorov-Arnold-Moser (KAM) curve in the phase space below the transition. According to [11] the FKM ground state is unique but in the pinned phase there are exponentially many stable configurations which are exponentially close to the ground state and the system resembles a fractal spin glass [12]. In the quantum FKM [13–15] the instanton tunneling between quasidegenerate configurations leads to a melting of the pinned instanton glass and the quantum phase transition into sliding phonon phase takes place above a critical value of the effective Planck constant $\hbar$ [16]. In contrast to the FKM with nearest neighbor interactions between particles, the ions have long range Coulomb interactions. In spite of that

[a] http://www.lpt.irsamc.ups-tlse.fr/∼dima

we show that the ion system is effectively described by the FKM and has similar phase transitions which can be studied experimentally. To analyze the properties of the FK Ion Model (FKIM) with few hundreds of ions we use various numerical methods including classical and Quantum Monte Carlo (QMC) algorithms as described in [12,13,16].

The structure of the paper is the following: in Section 2 we describe the FKI model and present the obtained results. The discussion of physical parameters and implementations is given in Section 3. Additional data for long ion chains are presented in Section 4 (Appendix).

2 The FKI model: description and results

The dimensionless FKIM Hamiltonian has the form:

$$H = \sum_{i=1}^{N} \left(\frac{P_i^2}{2} + \frac{\omega^2}{2} x_i^2 - K \cos x_i \right) + \sum_{i>j} \frac{1}{|x_i - x_j|} \quad (1)$$

where P_i, x_i are ion momentum and position, K gives the strength of optical lattice potential and all N ions are placed in a harmonic potential with frequency ω. To make a transfer from (1) to dimensional physical units one should note that the lattice constant d in $K\cos(x_i/d)$ is taken to be unity, the energy $E = H$ is measured in units of ion charge energy e^2/d and $\omega^2 \to m\omega^2 d^3/e^2$ where m is ion mass. In the quantum case $P_i = -i\hbar\partial/\partial x_i$ with dimensionless $\hbar$ measured in units $\hbar \to \hbar/(e\sqrt{md})$. In the quantum case we use the approximation of distinguishable ions which is well justified when the distance between ions imposed by the harmonic potential is comparable with the lattice period [2].

We start the discussion from the classical case. Here the stable configurations with minimal energy have $P_i = 0$ and satisfy the conditions $\partial H/\partial x_i = 0$. In approximation of only nearest neighbor interacting ions these conditions lead to the dynamical recursive map for equilibrium ion positions x_i:

$$p_{i+1} = p_i + Kg(x_i)\ , \quad x_{i+1} = x_i + 1/\sqrt{p_{i+1}}\ , \quad (2)$$

where the effective momentum conjugated to x_i is $p_i = 1/(x_i - x_{i-1})^2$ and the kick function $Kg(x) = -\omega^2 x - K\sin x$. To check the validity of this description we find the ground state configuration using numerical methods described in [11,12]. The harmonic frequency ω is chosen in such a way that in the middle of the chain the ion density $\nu = 2\pi/(x_1 - x_0)$ at $K = 0$ is equal to the golden mean value $\nu = \nu_g = (\sqrt{5}+1)/2$. This corresponds to an incommensurate phase with the golden KAM curve usually studied for the Aubry transition [10,11]. For a fixed $\nu \sim 1$ the strength of harmonic potential ω^2 drops with N according to relations found in [5,6]. The numerical values x_i allow to determine the function $g(x)$ using relations (2) and show that with good accuracy $g(x) = -\sin x$ (see Fig. 1). We attribute this result to an effective screening of global harmonic potential by long range interactions between ions in the central part of the chain where the ion density is approximately constant. For small values of optical potential ($K = 0.03$) the chain is in the sliding phase with a continuous KAM curve in the plane (p, x) while above the Aubry transition at $K = 0.2$ it is in the pinned phase and forms a fractal Cantor set in the phase space (Fig. 1). The qualitative change of chain properties is also seen via the hull function $h(x)$ which gives the ion positions in periodic potential vs. unperturbed positions at $K = 0$ both taken mod 2π: for $K < K_c$ one has a continuous function $h(x) \approx x$ while for $K > K_c$ the hull function has a form of devil's staircase with clustering of ion positions at certain values (Fig. 1). More data for a larger number of ions $N = 150$ are shown in Appendix (see Fig. 6).

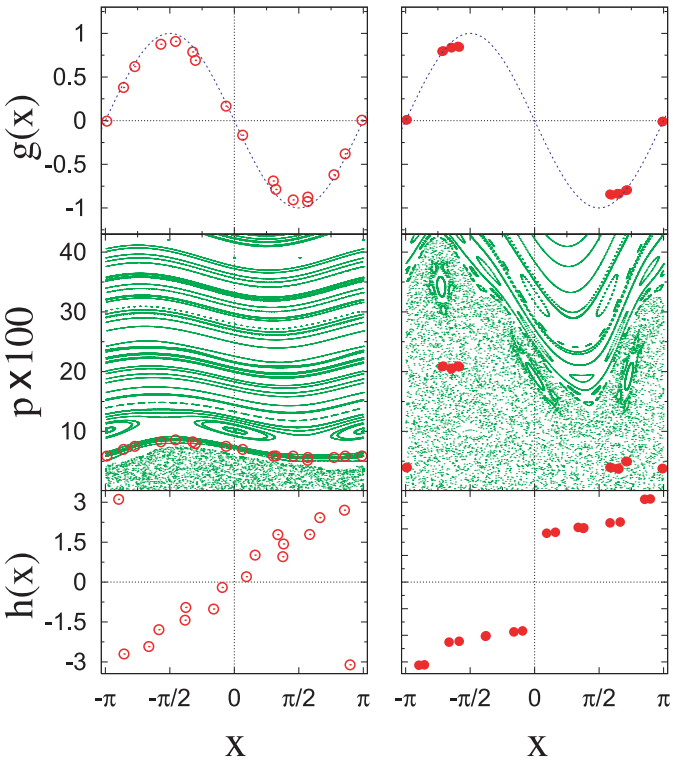

Fig. 1. (Color online) Functions related to the dynamical map (2) obtained from the ground state equilibrium positions x_i of $N = 50$ ions for $\omega = 0.014$ at $K = 0.03$ (open circles, left column) and $K = 0.2$ (full circles, right column). Panels show: the kick $g(x)$ function (top); the phase space (p, x) of the map (2) with $g(x) = -\sin x$ (green/gray points) and actual ion positions (red/black circles) (middle); the hull function $h(x)$ (bottom). The ion positions are shown as $x = x_i \pmod{2\pi}$ for the central 1/3 part of the chain.

The structural changes in the chain below and above the Aubry transition at the critical value K_c are also clearly seen in the spectrum of phonon excitations shown in Figure 2 (see also Fig. 7 in Appendix for $N = 150$). For $K < K_c$ the spectrum of phonon modes has a sound like form at small wave vectors k, going down to a minimal oscillation frequency $\omega_0 \approx \omega$, which is small compared to frequencies of periodic potential. For $K > K_c$ the spectrum of excitations is characterized by a phonon gap when

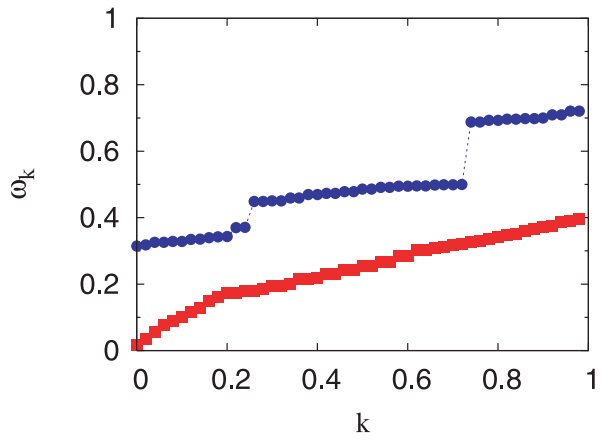

Fig. 2. (Color online) Phonon spectrum $\omega(k)$ as a function of scaled mode number $k = i/N$ $(i = 0, \ldots, N-1)$, for $K = 0.03$ (bottom curve, squares) and $K = 0.2$ (top curve, points) for the case of Figure 1.

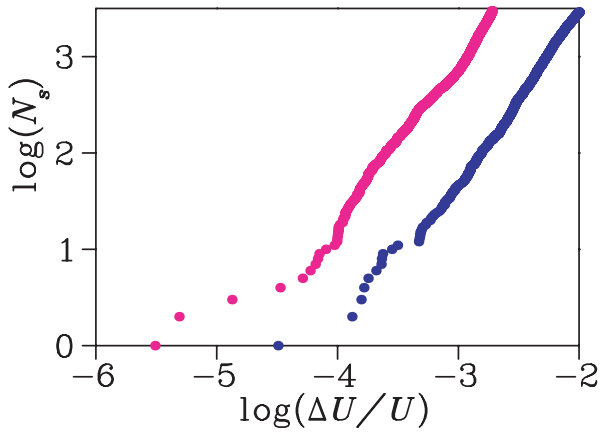

Fig. 4. (Color online) Number of equilibrium configurations N_s as a function of their relative excitation energy $\Delta U/U$ above the ground state for 50 (blue/black) and 150 (magenta/gray) ions at $K = 0.2$ with ω as in Figure 3 (logarithms are decimal).

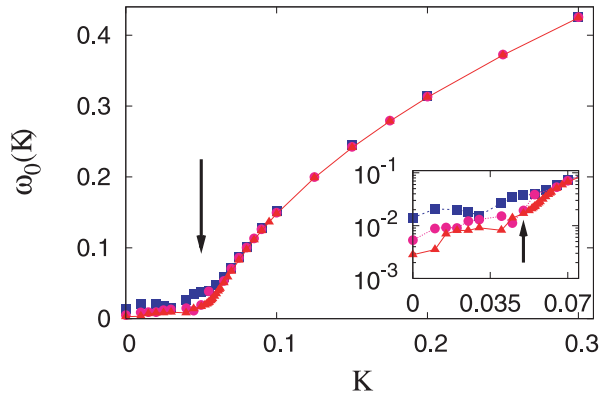

Fig. 3. (Color online) Minimal excitation frequency $\omega_0(K)$ as a function of periodic potential strength K for the golden mean ion density ν_g and number of ions $N = 50$ (squares; $\omega = 0.014$), $N = 150$ (circles; $\omega = 0.00528$), $N = 300$ (triangles, $\omega = 0.00281$). The critical point $K_c \approx 0.05$ is marked by arrow; inset shows data near K_c.

ω_0 becomes independent of number of ions N (Fig. 3). According to the data of Figure 3 for $\omega_0(K)$ and of Figure 8 in Appendix for the hull function the critical point is located at $K_c \approx 0.05$. The value K_c can be obtained approximately by a reduction of map (2) to the Chirikov standard map [17]. For that the second equation (2) can be linearized near $1/\sqrt{p} = 2\pi/\nu_g$ that gives the Chirikov standard map with chaos parameter $K_{eff} = K(2\pi/\nu_g)^3/2$ and the critical value $K_c = 0.034$ corresponding to $K_{eff} = 1$. This value is smaller than the value $K_c \approx 0.05$ obtained from numerical data that can be attributed to a strong dependence of K_{eff} on ν_g.

The obtained results show that the ion chain in a periodic potential has close similarities with the FKM. The map (2) describes quite accurately the central 1/3 part of the chain where the ion density is approximately constant. Outside of this part the ion density starts to grow and deviations from the map start to be visible in (p, x) plain and $h(x)$, even if the g-function remains rather close to $g = -\sin x$. A separation on two parts is also seen in the lowest phonon eigenmodes which are localized in the central part of the chain (see Figs. 9, 10 of Appendix). Also, in similarity with the FKM [12], we find that in the pinned phase at $K > K_c$ the FKIM has properties of a spin glass with enormous number of stable equilibrium configurations N_s in the very close vicinity of the ground state (see Fig. 4).

These quasidegenerate configurations become very important in the quantum chain where quantum tunneling between them leads to nontrivial instanton excitations. To study the quantum case we use the QMC approach [13,16,18] with the Euclidean time τ in the interval $[0, \tau_0]$ and system temperature $T = \hbar/\tau_0$. We use large values of τ_0 (e.g. $\tau_0 \geq 400$) so that the temperature T is small compared to periodic potential K and phonon gap $\hbar\omega_0$. To see the structural changes produced by quantum fluctuations it is convenient to compute the formfactor of ion positions defined as $F(k) = \langle \sum_i \left| \exp(ikx_i(\tau)) \right|^2 \rangle / \delta N$, where summation is taken over the central part of the chain with $\delta N \approx N/3$ ions, $x_i(\tau)$ are ions positions at Euclidean time τ and brackets mark averaging over τ. In the classical case x_i are the equilibrium positions of ions. For $\hbar = 0$ the formfactor peaks are equidistant in ν_g that clearly show the incommensurate sliding phase at $K = 0.03 < K_c$ (Fig. 5a). For $K = 0.2 > K_c$ the peaks in $F(k)$ are at integer k values showing that ions are pinned by the optical lattice (Fig. 5b bottom). In the quantum case at $K = 0.2 > K_c$ and small values of $\hbar = 0.1$ the density of instantons is small and quantum tunneling does not destroy the pinned phase. However, at large $\hbar = 2$ quantum fluctuations lead to melting of pinned phase, the integer peaks disappear and $F(k)$ becomes continuous (Fig. 5b). This means that the ion chain can slide in the optical lattice. The quantum phase transition from pinned instanton glass to sliding phonon gas takes place at zero temperature and certain $\hbar_c \sim 1$.

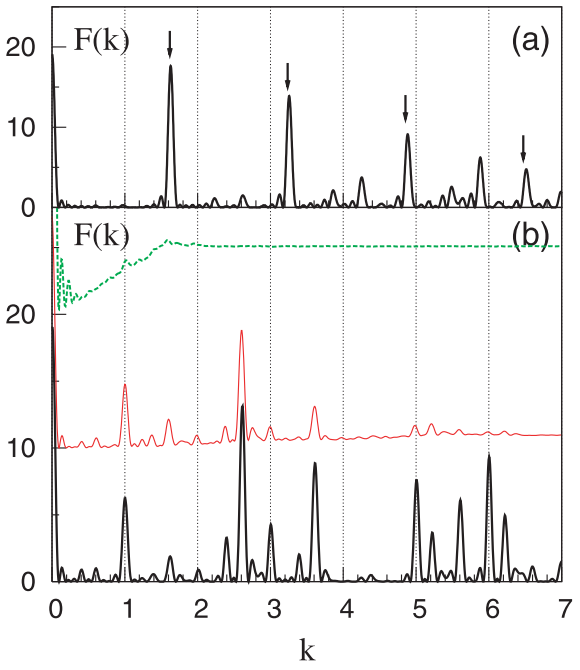

Fig. 5. (Color online) Formfactor $F(k)$ (see text) of the chain with $N = 50$ ions and $\omega = 0.014$. (a) The classical incommensurate phase at $K = 0.03$, $\hbar = 0$, arrows mark the peaks at integer multiples of golden mean density ν_g. (b) The pinned phase case at $K = 0.2$ for $\hbar = 0$ (bottom black curve), $\hbar = 0.1$ (middle red curve shifted 10 units upward), $\hbar = 2$ (top green curve shifted 20 units upward, for clarity $F(k)$ is multiplied by factor 5). The temperature of the quantum chain is $T = \hbar/\tau_0$ with $\tau_0 = 400$ so that $T \ll K$ and $T \ll \hbar\omega_0(K)$.

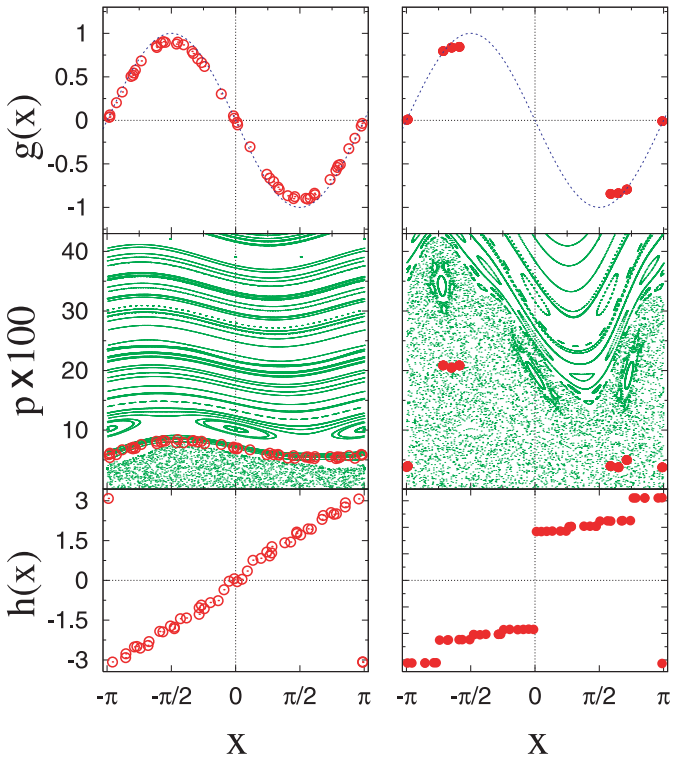

Fig. 6. (Color online) Same as in Figure 1 but for $N = 150$ ions at $\omega = 0.00528$ corresponding to the golden mean density of ions in the middle of the chain (compare with data of Fig. 2 for $N = 50$).

3 Discussion

Let us now discuss the physical parameters needed for experimental investigations of the ion chains in optical lattices.

For experimental conditions like in [3] the distance between Ca ions is about $\Delta x \approx 5$ μm so that the golden mean density ν_g corresponds to the lattice constant $d = \nu_g \Delta x/2\pi \approx 1.3$ μm. This value can be realized by laser beams crossed at a fixed angle. The transition to pinned phase takes place at the optical lattice potential $V = K_c e^2/d \approx 0.6K$ that in principle can be reached in strong laser fields. For $^{40}Ca^+$ ions with such d the dimensionless Planck constant is $\hbar_{eff} = \hbar/(e\sqrt{md}) \approx 3 \times 10^{-5}$. This means that such experiments with cold trapped ions can be performed in a deep semiclassical regime hardly accessible to the QMC numerical simulations. We also note that a strong gap in phonon spectrum ω_k for $K > K_c$ (Figs. 2 and 3) may be useful for protection of quantum gate operations in quantum computations.

Various phases of the FKI model can seen with the help of the formfactor $F(k)$ as it is shown in Figures 5 and 11. The formfactor $F(k)$ can be experimentally obtained by light scattering on the ion chain and in this way various phases of the system can be detected. Experimental studies with ions in optical lattice will allow to detect the transition between pinned to sliding phases and investigate it in a deep semiclassical regime hardly accessible for numerical simulations.

Another physical realization of the FKI model can be obtained by replacing ions with electrons and placing their chain (the Wigner crystal) in a periodic potential. In this case higher values of dimensionless $\hbar$ can be reached with $\hbar \approx 0.1$ for $d \approx 5$ nm. Such a situation may appear in 1D electron wires, molecular structures or nanotubes where a devil's staircase behavior has been discussed recently [19]. In the regime when the number of electrons per period is of the order of $\nu \sim 1$ the effects related to statistics of particles are not so crucial and the quantum melting of the pinned phase should qualitatively follow the scenario described here. Hence, the obtained results describe also a more general problem of a Wigner crystal in a periodic potential.

This work was supported in part by the EC IST-FET project EuroSQIP.

4 Appendix

Here in Figures 6–11 we present additional data showing results with larger number of ions with up to 150 ions. In general they confirm the conclusions obtained with chains of 50 ions (see Figs. 1–5). Thus, experimental studies with about 50 ions should allow to see main physical effects present in much longer chains.

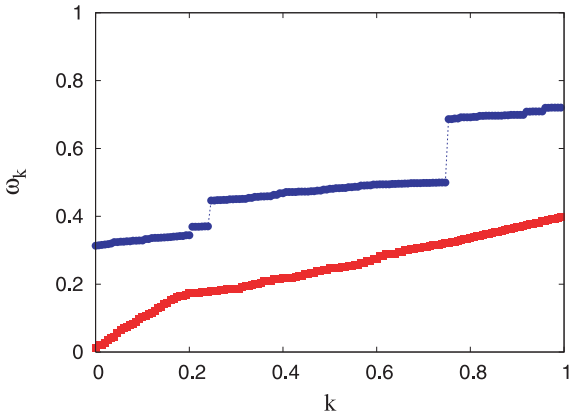

Fig. 7. (Color online) Phonon spectrum $\omega(k)$ as a function of scaled mode number $k = i/N$ $(i = 0, \ldots, N-1)$, for $K = 0.03$ (bottom curve, squares) and $K = 0.2$ (top curve, points) for the case of Figure 6 at $N = 150$ (compare with data of Fig. 2 for $N = 50$).

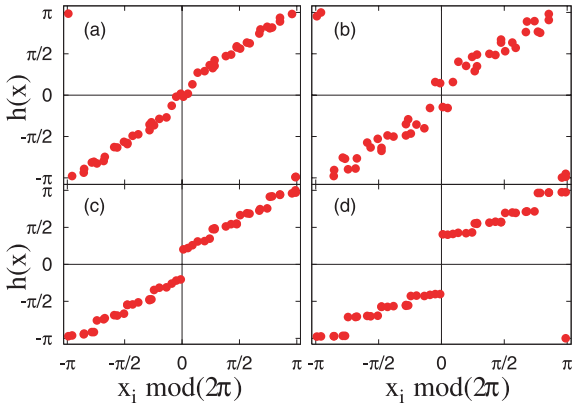

Fig. 8. (Color online) Evidence of the Aubry transition in the hull function. The hull function $h(x)$ shows the ion positions $x_i(K)$ mod (2π) in presence of periodic potential as a function of ion positions $x_i^{(0)}$ mod(2π)) without potential $(K = 0)$. Here $N = 150$, $\omega = 0.000528$, (a) $K = 0.04$; (b) $K = 0.055$; (c) $K = 0.065$; (d) $K = 0.1$. Only the central 1/3 part of the chain is shown (compare with data of Fig. 1 (bottom) shown for 50 ions).

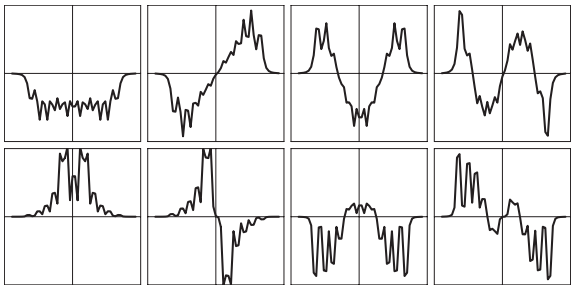

Fig. 9. Phonon eigenmodes in the chain with $N = 50$ ions at the golden mean ion density with $\omega = 0.014$. Panels show the amplitude of eigenmode (in arbitrary linear units) vs. ion positions x_i varied from minimal to maximal value for lowest 4 modes with number 0, 1, 2, 3 (from left to right). Top row is for $K = 0.03$ and bottom row is for $K = 0.2$.

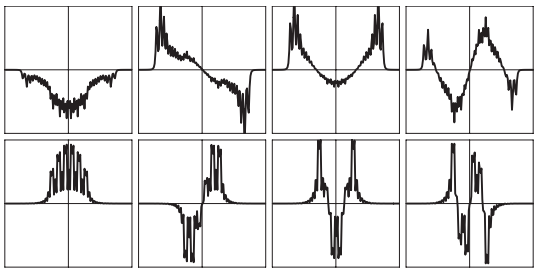

Fig. 10. Same as in Figure 9 for $N = 150$, $\omega = 0.00528$.

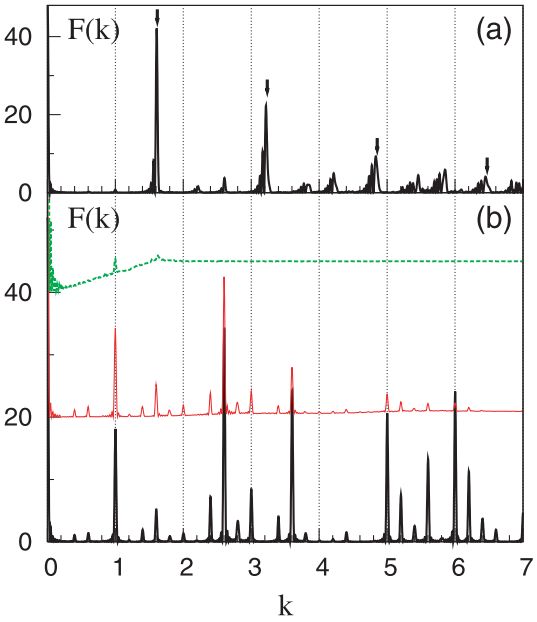

Fig. 11. (Color online) Formfactor $F(k)$ (see text) of the chain with $N = 150$ ions and $\omega = 0.00528$. (a) The classical incommensurate phase at $K = 0.03$, $\hbar = 0$, arrows mark the peaks at integer multiples of golden mean density ν_g. (b) The pinned phase at $K = 0.2$ for $\hbar = 0$ (bottom black curve), $\hbar = 0.1$ (middle red curve shifted 20 units upward), $\hbar = 2$ (top green curve shifted 40 units upward, for clarity $F(k)$ is multiplied by factor 5). The temperature of the quantum chain is $T = \hbar/\tau_0$ with $\tau_0 = 400$ so that $T \ll K$ and $T \ll \hbar\omega_0(K)$. (Compare with data of Fig. 5 for $N = 50$).

References

1. G. Birkl, S. Kassner, H. Walther, Nature **357**, 310 (1992)
2. J.I. Cirac, P. Zoller, Phys. Rev. Lett. **74**, 4091 (1995)
3. H. Häffner, W. Hänsel, C.F. Roos, J. Benhelm, D. Chek-al-kar, M. Chwalla, T. Körber, U.D. Rapol, M. Riebe, P.O. Schmidt, C. Becher, O. Gühne, W. Dür, R. Blatt, Nature **438**, 643 (2005)
4. D. Leibfried, E. Knill, S. Seidelin, J. Britton, R.B. Blakestad, J. Chiaverini, D.B. Hume, W.M. Itano, J.D. Jost, C. Langer, R. Ozeri, R. Reichle, D.J. Wineland, Nature **438**, 639 (2005)
5. D.H.E. Dubin, T.M. O'Neil, Rev. Mod. Phys. **71**, 87 (1999)
6. G. Morigi, S. Fishman, Phys. Rev. Lett. **93**, 170602 (2004)
7. O. Morsch, M. Oberthaler, Rev. Mod. Phys. **78**, 179 (2006)
8. H. Katori, S. Schlipf, H. Walther, Phys. Rev. Lett. **79**, 2221 (1997)

9. Ya.I. Frenkel, T.A. Kontorova, Zh. Eksp. Teor. Fiz. **8**, 1340 (1938) [Phys. Z. Sowjetunion **13**, 1 (1938)]
10. O.M. Braun, Yu.S. Kivshar, *The Frenkel-Kontorova Model: Concepts, Methods, Applications* (Springer-Verlag, Berlin, 2004)
11. S. Aubry, Physica D **7**, 240 (1983)
12. O.V. Zhirov, G. Casati, D.L. Shepelyansky, Phys. Rev. E **65**, 026220 (2002)
13. F. Borgonovi, I. Guarneri, D.L. Shepelyansky, Phys. Rev. Lett. **63**, 2010 (1989)
14. G.P. Berman, E.N. Bulgakov, D.K. Campbell, Phys. Rev. B **49**, 8212 (1994)
15. B. Hu, B. Li, W.M. Zhang, Phys. Rev. E **58**, R4068 (1998)
16. O.V. Zhirov, G. Casati, D.L. Shepelyansky, Phys. Rev. E **67**, 056209 (2003)
17. B.V. Chirikov, Phys. Rep. **52**, 263 (1979)
18. M. Creutz, B. Freedman, Ann. Phys. (N.Y.) **132**, 427 (1981)
19. D.S. Novikov, Phys. Rev. Lett. **95**, 066401 (2005)